Spontaneous Emission Suppression via Quantum Path Interference in Coupled Microcavities

M. M. Dignam,[1,*] D. P. Fussell,[1] M. J. Steel,[2,1] C. Martijn de Sterke,[1] and R. C. McPhedran[1]

[1]*Centre for Ultrahigh bandwidth Devices for Optical Systems (CUDOS), School of Physics, University of Sydney 2006, Australia*

[2]*RSoft Design Group, Inc., 65 O'Connor Street, Chippendale, New South Wales 2008, Australia*

(Received 30 March 2005; revised manuscript received 23 December 2005; published 16 March 2006)

We examine theoretically the spontaneous emission rate in optical microstructures with cavity resonances that overlap in both position and frequency. Using projection techniques, we show that the spontaneous emission in such structures can be accurately described by the direct emission and quantum path interference of emission into a few discrete resonant modes, even though the exact infinite-dimensional problem involves a coupling to the continuum of radiation states. Moreover, we obtain an efficient numerical time-domain method for determining the spontaneous emission rate that incorporates these effects, including the suppression of spontaneous emission into some modes.

DOI: 10.1103/PhysRevLett.96.103902 PACS numbers: 42.70.Qs, 41.20.−q, 42.25.Fx

A central goal of photonic microcavity research is to modify and control the spontaneous emission (SE) properties of atoms and quantum dots by tailoring the resonances in these structures. Most work in this area has focused either on simple single-resonance cavities [1–6] or on photonic crystals (PCs) [4,7–10]. In these structures, the SE rate can either be enhanced or suppressed depending on the structure and the emitter location.

For structures with a *single well-isolated resonance* at, say, $\omega = \omega_m$, the ratio $R_{\mathrm{SE}}(\omega_a, \mathbf{r}_a)$ of the rate of SE from an atom in a microstructure at $\mathbf{r} = \mathbf{r}_a$ with transition frequency ω_a to that of the same atom in vacuum, can be expressed simply as [3,11]

$$R_{\mathrm{SE}}(\omega_a, \mathbf{r}_a) = \frac{3c\lambda^2 \rho_m(\omega_a)}{4n^3(\mathbf{r}_a) V_m(\mathbf{r}_a)}, \tag{1}$$

where c is the speed of light in vacuum, $V_m(\mathbf{r}_a)$ is the effective mode volume [3], $\lambda = 2\pi c/\omega_a$ is the wavelength of the radiation, $n(\mathbf{r}_a)$ is the refractive index at the location of the atom, and $\rho_m(\omega)$ is the line shape function. For an isolated resonance, $\rho_m(\omega)$ is a normalized Lorentzian with central frequency ω_m and quality factor Q_m. The maximum SE ratio is the Purcell factor, F_{P}, obtained by optimizing the dipole orientation and the atom location $\mathbf{r}_a$ to yield the well-known result [3,12] $F_{\mathrm{P}} = 3\lambda^3 Q_m/[4\pi^2 n(\mathbf{r}_a)^3 V_{\min}]$, where $V_{\min}$ is the minimized effective mode volume.

The simple parametrization of the SE ratio in Eq. (1) is physically appealing as it describes a complicated open system in terms of the properties of a single resonance. For structures like coupled microcavities with *multiple resonances*, this approach can be generalized by summing over the resonances as long as the resonances do not simultaneously overlap in both frequency and space. However, for structures with resonances that do overlap in both frequency and space (''overlapping resonances''), such a simple expression is, in general, not possible.

In this Letter, we derive a physically transparent expression for the SE ratio in *finite* dielectric microstructures with *open boundaries and overlapping resonances* by projecting the local density of states onto a suitable set of discrete modes. For convenience, we use the truly discrete modes of a closely related *closed* structure, but this is not required. This simplified expression for R_{SE} not only contains terms as in Eq. (1), but also new, qualitatively different terms describing *quantum path interference (QPI)* of the SE into different quasimodes. We demonstrate the accuracy of our simple expression for R_{SE} and use it to quantify the effects of QPI on SE in coupled dielectric microcavities, including the probability of photon emission into a given quasimode. We use this approach to develop an efficient and general numerical method to calculate R_{SE} in these complex situations.

To illustrate our approach, we model the TM modes $[\mathbf{E}_m(\mathbf{r}, t) = E_m(\mathbf{r}, t)\hat{z}]$ of the 2D PC, shown in Fig. 1, consisting of a *finite* square array (period d) of cylinders in air. The cylinders are infinite, with radius, $R = 0.13d$, and refractive index $n = 3$. The structure has open boundaries

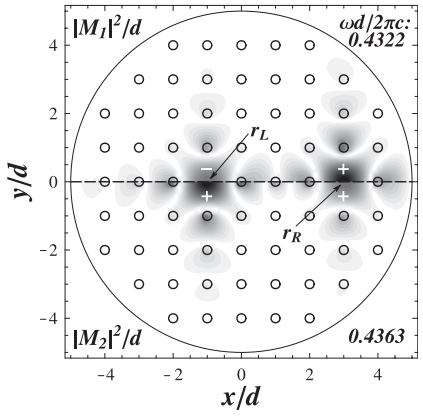

FIG. 1. Index of refraction and intensity profile for the two modes in the lowest band gap. As the modes are symmetric about $y = 0$, $|\mathbf{M}_1(\mathbf{r})|^2$ ($|\mathbf{M}_2(\mathbf{r})|^2$) is only shown for $y > 0$ ($y < 0$). Small circles denote the rods, while the large circle encloses volume, V_s, and denotes the hard boundary used to calculate the quasimodes.

and two asymmetrically placed defect microcavities. We work at frequencies inside the lowest band gap of this structure: $\omega \in [2.5446, 3.0758]c/d$.

The SE ratio for an atom with transition dipole, $\mathbf{d} = \mu\hat{e}_k$, for any structure can be rigorously expressed as [5,13]

$$R_{\mathrm{SE}}(\omega_a;\mathbf{r}_a) = \frac{3\pi^2c^3}{n_s\omega_a^2}L_k(\omega_a;\mathbf{r}_a), \tag{2}$$

where $L_k(\omega;\mathbf{r})$ is the local density of states (LDOS) at $\mathbf{r}$. The LDOS gives the spectral density of modes versus position and can be expressed as a modal expansion or directly in terms of the Green tensor, $\mathbf{G}$, as $L_k(\omega;\mathbf{r}) = -2\omega\,\mathrm{Im}\{G_{kk}(\omega;\mathbf{r},\mathbf{r})\}/\pi c^2$, where $\mathbf{G}$ satisfies the usual inhomogeneous Helmholtz equation [13]. We have calculated the LDOS using the Rayleigh-multipole method [13] and plot $L_z(\omega;x,y=0)$ for our 2D PC in Fig. 2. The LDOS has large resonances near the centers of the two defects but with very different behavior in the two defects: there is a large sharp spectral peak at the center of the left defect but a much smaller peak with a deep spectral dip at the center of the right defect. As shown below, this strong asymmetry, and the spectral dip, in particular, are the result of QPI.

We generalize Eq. (1) by introducing the *reduced* LDOS associated with a finite number of resonances. The true modes, $\mathbf{f}_\gamma(\mathbf{r})$, of a *finite, open* dielectric microstructure extend over all space and form a continuum labeled by γ. However, it is exceedingly difficult to use such modes to compute or understand the SE in the microstructure, and it would be far preferable to employ the *cavity resonances* as was done in Eq. (1). In practice, high-Q resonances always have a much larger field amplitude within some relatively small volume, V_s, than elsewhere. For such resonances, the field is almost unchanged within volume V_s if we enclose it by an appropriate perfectly reflecting boundary (cf. Fig. 1) [14]. The modes, $\mathbf{M}_m(\mathbf{r})$, of this related *finite and closed* structure, which vanish outside V_s, are *discrete*, and can be

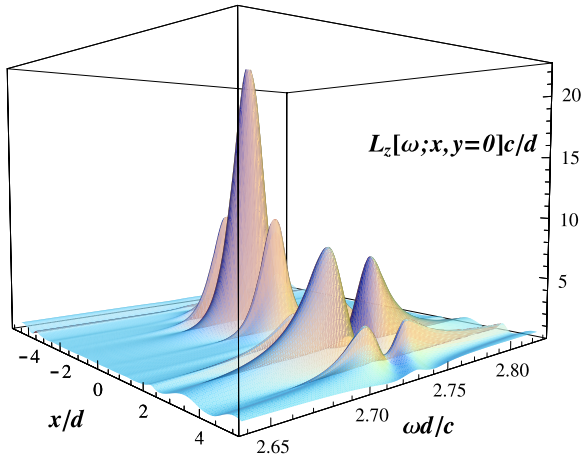

FIG. 2 (color online). LDOS for the structure of Fig. 1 evaluated at $y = 0$ as a function x and ω.

chosen to be real and orthonormal: $\int d^3\mathbf{r}n^2(\mathbf{r})\mathbf{M}_m(\mathbf{r})\cdot\mathbf{M}_n(\mathbf{r}) = \delta_{m,n}$.. These *quasimodes* are not true modes of the *open* system; they can be expanded exactly in terms of the true extended modes of the open system as

$$\mathbf{M}_m(\mathbf{r}) = \int d\gamma g_\gamma^m \mathbf{f}_\gamma(\mathbf{r}), \tag{3}$$

with expansion coefficients $g_\gamma^m = \int d^3\mathbf{r}n^2(\mathbf{r})\mathbf{f}_\gamma^*(\mathbf{r})\cdot\mathbf{M}_m(\mathbf{r})$. We calculated the two TM quasimodes in the lowest band gap of our PC for the boundary shown in Fig. 1 and plot $|\mathbf{M}_m(\mathbf{r})|^2$ in Fig. 1. The modes overlap in space and are close in frequency.

We define the *reduced* LDOS as the projection of the LDOS onto the subspace spanned by the quasimodes of interest, $\mathbf{M}_m(\mathbf{r})$. Here we assume there are two such modes with $m = \{1, 2\}$, noting that the generalization to the multimode case is straightforward. Thus obtaining the reduced LDOS and using Eq. (2) we find the reduced spontaneous emission ratio,

$$R_{\mathrm{SE}}^{(2)}(\omega_a,\mathbf{r}_a) = \frac{3c\lambda^2\rho_1(\omega_a)}{4n^3(\mathbf{r}_a)V_1(\mathbf{r}_a)} + \frac{3c\lambda^2\rho_2(\omega_a)}{4n^3(\mathbf{r}_a)V_2(\mathbf{r}_a)} + \frac{3c\lambda^2[\hat{e}_k\cdot\mathbf{M}_1(\mathbf{r}_a)][\hat{e}_k\cdot\mathbf{M}_2(\mathbf{r}_a)]\,\mathrm{Im}\{C_{12}(\omega)\}}{2n(\mathbf{r}_a)}, \tag{4}$$

where

$$C_{mp}(\omega) \equiv -\frac{2\omega}{\pi c^2}\int d^3\mathbf{r}\int d^3\mathbf{r}'n^2(\mathbf{r})n^2(\mathbf{r}')\mathbf{M}_m(\mathbf{r})\cdot\mathbf{G}(\omega;\mathbf{r},\mathbf{r}')\cdot\mathbf{M}_p(\mathbf{r}') \tag{5}$$

and $\rho_m(\omega) \equiv \mathrm{Im}\{C_{mm}(\omega)\}$. Finally, the effective mode volume, $V_m(\mathbf{r}_a)$, for an atom at $\mathbf{r}_a$ is given by [3] $[V_m(\mathbf{r}_a)]^{-1} \equiv n^2(\mathbf{r}_a)[\hat{e}_k\cdot\mathbf{M}_m(\mathbf{r}_a)]^2$.

The factor $C_{mp}(\omega)$ has a simple physical interpretation: it is the Fourier transform of the probability amplitude for finding radiation in mode p given that it was initially in mode m. That is, using a modal expansion of the Green function [13], we have $C_{mp}(\omega) = \int_0^\infty dt c_{mp}(t)e^{i\omega t}$, where

$$c_{mp}(t) \equiv -2i\int d^3\mathbf{r}n^2(\mathbf{r})\mathbf{M}_p(\mathbf{r})\cdot[\mathbf{E}^+(\mathbf{r},t)/E_o]^*, \tag{6}$$

and $\mathbf{E}^+(\mathbf{r},t)$ is the positive frequency part of the electric field in the structure with the initial condition, $\mathbf{E}^+(\mathbf{r},t=0) = E_o\mathbf{M}_m(\mathbf{r})$. Thus, $C_{mm}(\omega)$ gives the decay dynamics of light out of mode m, while $C_{12}(\omega)$ gives the decay dynamics from mode 1 to mode 2.

The first two terms in Eq. (4) simply give the direct contributions from the two resonances as in Eq. (1). The third *interference* term describes the dynamics of radiation transfer between the two modes. If the resonances are overlapping resonances then the third term can be important and R_{SE} cannot be written as a sum over terms as in Eq. (1); we must use either the full LDOS or Eq. (4). We stress that the mode coupling is not simply an artifact of choosing an inappropriate two-mode basis; it is easily proven that it is impossible to model the spontaneous emission rate at all points inside such a system accurately using only the first two terms in Eq. (4), regardless of the

form chosen for the modes or their line shapes. Thus, in any two-mode representation of the resonances, there is always radiation transfer between the two modes. We find that very accurate results are obtained throughout most of the structure if we choose the quasimodes to be the modes of the closed structure with the boundary roughly 0.2λ to 0.4λ from the edge of the structure [14].

One would not normally use Eq. (5) to calculate the $C_{mp}(\omega)$ as it requires the full Green tensor inside the structure, which is precisely the quantity we are after. Instead, the $C_{mp}(\omega)$ can be simply and efficiently obtained using a finite-difference time-domain (FDTD) approach to calculate the time evolution of the field in the open structure with initial condition $\mathbf{E}^+(\mathbf{r}, t = 0) = E_o\mathbf{M}_m(\mathbf{r})$. This field is then used in (6) to calculate $c_{mp}(t)$ which yields $C_{mp}(\omega)$ as its positive-time Fourier transform. Thus, calculating the spontaneous emission rate (or LDOS) at all points that are not too near the boundary and at all frequencies close to the resonant frequencies only requires two FDTD calculations; a vast improvement on standard FDTD calculation of the Green tensor [15,16] that requires a separate FDTD for every point in space (typically $\gtrsim 500$ points), making our method at least 2 orders of magnitude faster.

In Fig. 3(a), we plot $\rho_1(\omega)$, $\rho_2(\omega)$, and $\mathrm{Im}\{C_{12}(\omega)\}$ for our structure calculated using the FDTD method. To confirm the accuracy, we also plot the results using Eq. (5) with the full Green tensor calculated using the multipole method [13]. The agreement is clearly excellent apart from a small frequency shift in the FDTD results by $\Delta\omega = 0.0044c/d$. Such a shift is typical in FDTD calculations and can be reduced by using a finer grid.

Because the resonances of this open structure are well described by the quasimodes $\mathbf{M}_1(\mathbf{r})$ and $\mathbf{M}_2(\mathbf{r})$ and the coupling between modes is not too strong, the $\rho_m(\omega)$ are very close to Lorentzian, with resonant frequencies ω_m and quality factors, Q_m. The deviation from Lorentzian line shape arises because the modes are not just coupled to a continuum, but also have significant coupling to each other. Note that $\mathrm{Im}\{C_{12}(\omega)\}$ is comparable in magnitude to the $\rho_m(\omega)$ and so is not a small correction. From Figs. 1 and 3(a) and using Eq. (4), it is now easy to understand Fig. 2. The modes have opposite signs near the left defect and the same sign near the right defect (see Fig. 1). Thus, the interference term in Eq. (4) is negative (destructive interference) at the right defect for $\omega \simeq 2.73c/d$, resulting in a large dip in the LDOS near this frequency. Similarly, the interference term at the left defect is positive (constructive interference) at this frequency, resulting in an enhanced LDOS peak.

The effect of the interference term is seen clearly in Fig. 3(b), where we plot the exact SE ratio, $R_{\mathrm{SE}}(\omega, \mathbf{r}_{L,R})$, versus frequency at the center of the left $[\mathbf{r}_L = (x_L, 0)]$ and right $[\mathbf{r}_R = (x_R, 0)]$ defect for $\hat{e}_k = \hat{z}$. Also shown is the reduced SE ratio, $R^{(2)}_{\mathrm{SE}}(\omega, \mathbf{r}_{L,R})$, calculated using Eq. (4) with FDTD, showing that the reduced LDOS is an excellent approximation to the exact LDOS near the defects. Note that to aid in comparison, we have removed the small frequency offset mentioned earlier. Figure 3(b) also shows $R^{(NI)}_{\mathrm{SE}}(\omega, \mathbf{r}_{L,R})$, which does not include the interference term in Eq. (4). Note that in the right defect, the interference term produces a large dip in the SE rate at $\omega = 2.734c/d$ which reduces the SE rate at dip center by a factor of 7.3 from its value without this term.

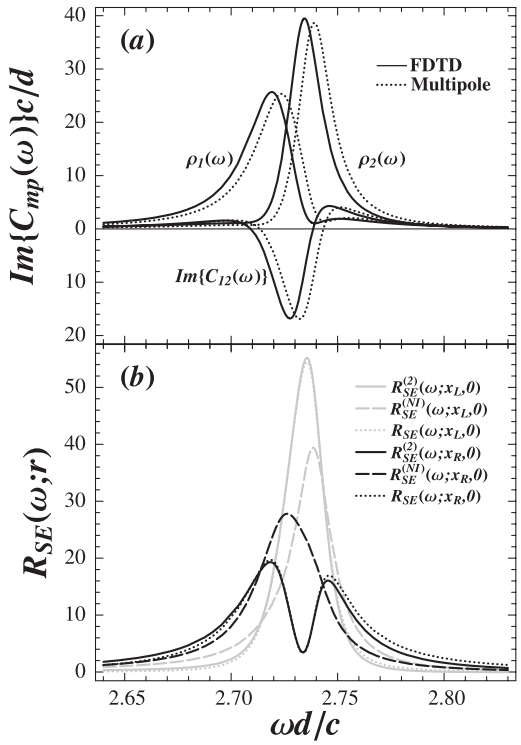

FIG. 3. (a) Quantities $\rho_1(\omega)$, $\rho_2(\omega)$, and $\mathrm{Im}\{C_{12}(\omega)\}$ for the two modes in Fig. 1 calculated using FDTD (solid lines) and Eq. (5) (dotted lines). (b) SE ratio $[R_{\mathrm{SE}}(\omega, \mathbf{r})]$, the reduced SE ratio $[R^{(2)}_{\mathrm{SE}}(\omega, \mathbf{r})]$, and the reduced SE ratio without the interference term $[R^{(NI)}_{\mathrm{SE}}(\omega, \mathbf{r})]$ at the centers of the two defects as a function of frequency. For comparison purposes, $R^{(2)}_{\mathrm{SE}}(\omega, \mathbf{r})$ has been frequency-shifted by the frequency difference found in Fig. 3(a).

We now turn to the quantum interpretation of the interference in the SE rate and the calculation of the probability of emission into the different quasimodes. For a two-level atom initially in state $|1; 0\rangle$ (atom in excited state; no photons), coupled to the continuum of single-photon states $|0; f_\gamma\rangle$ [atom in ground state; single photon in mode $\mathbf{f}_\gamma(\mathbf{r})$], the state of the system at time t can be written as $|\psi(t)\rangle = \alpha(t)|1;0\rangle + \int d\gamma\beta(\gamma;t)|0;f_\gamma\rangle$, where the temporal Fourier transform of $\beta(\gamma; t)$ is given by $\bar{\beta}(\gamma;\omega) = i\sqrt{\omega_\gamma/2\hbar\epsilon_0}\mathbf{d}^* \cdot \mathbf{f}^*_\gamma(\mathbf{r}_a)\bar{\alpha}(\omega)/[\omega - \omega_\gamma]$, where ϵ_0 is the permittivity of free space and $\bar{\alpha}(\omega)$ is the Fourier transform of $\alpha(t)$, given by $\bar{\alpha}(\omega) = i/[\omega - \omega_a - W(\omega)]$, where $W(\omega)$ is the *shift-width function* [4]. From Eq. (3), the quantum state associated with the nonstationary quasimode $\mathbf{M}_m(\mathbf{r})$ of the open structure can be expanded as $|0; M_m\rangle = \int d\gamma g^m_\gamma|0; f_\gamma\rangle$. To

obtain the probability of finding the system in state $|0; M_m\rangle$, we project the state function $|\psi(t)\rangle$ onto $|0; M_m\rangle$. Using the expressions for $\bar{\beta}(\gamma; \omega)$ and for the reduced LDOS, the Fourier transform of the probability amplitude for finding the system in state $|0; M_1\rangle$ is

$$\bar{B}_1(\omega) = -\sqrt{\frac{\omega_a}{2\hbar\epsilon_o}}\frac{2\omega_a}{c^2[\omega - \omega_a - W(\omega)]} \times [C_{11}(\omega)\mathbf{M}_1(\mathbf{r}_a) + C_{12}(\omega)\mathbf{M}_2(\mathbf{r}_a)] \cdot \mathbf{d}^*. \quad (7)$$

The first term in this expression gives the probability amplitude for the direct decay of the atom into mode 1, while the second gives the probability amplitude for decay into mode 2 and subsequent transfer into mode 1. Thus, there are two quantum paths to reach state $|0; M_1\rangle$ and these two paths interfere constructively or destructively depending on the atom's position and transition frequency. As the relaxation of the atom into the ground state is dominated by emission into the resonant modes ($m = \{1, 2\}$), the SE ratio reflects this QPI via the third term in Eq. (4). We therefore see that the large dip in the SE rate for atoms in the right defect is due to the quantum interference between two paths for the SE of the atom into the resonant modes of the structure.

It could be argued that QPI is an integral part of the modification of the SE rate in *any* cavity, or even for an atom placed close to a mirror. This is true in that it is interference of the free-space radiation modes that results in the formation of the resonant modes of a cavity. However, there is a qualitative difference between this and the QPI discussed here. In a general microcavity system, the QPI arises out of a complex interference between *many continuum free-space modes* and cannot be accurately modeled using only a *few* of these modes. In contrast the QPI discussed here is the interference arising between a few *quasimodes*; the QPI between these few quasimodes describes and explains the key features of the SE dynamics of the system.

Because of the simplicity of the projected LDOS, it is easy to see how the interference can be manipulated not only to alter the SE rate at a given position, but also to control the SE rate into a given quasimode. In the weak-coupling regime, the SE rate of the atom is much slower than the decay rate of light out of the modes. Using Eq. (7), we then find that for $t > \tau_m$ (where $\tau_m \equiv Q_m/\omega_m$ is the quasimode lifetime), the probability of finding the photon in quasimode m in a structure that is well described by N quasimodes is given approximately by

$$P_m(t) \simeq Ae^{-\Gamma_{\mathrm{SE}}t}\left|\sum_{p=1}^{N} C_{mp}(\omega_a)\mathbf{M}_p(\mathbf{r}_a)\cdot\mathbf{d}^*\right|^2, \quad (8)$$

where A is independent of m, and $1/\Gamma_{\mathrm{SE}}$ is the SE lifetime. Thus, the probability of emission into a given quasimode can be easily determined from the $\mathbf{M}_m(\mathbf{r})$ and $C_{mp}(\omega)$ that make up our projected LDOS and $R_{\mathrm{SE}}^{(2)}$. By changing the structure or the emitter position slightly, the QPI can be altered so as to reduce or enhance the emission into a particular mode. Thus, our reduced LDOS makes it possible for us to see how to tailor the emission into individual quasimodes.

The numerical results presented here are for a 2D structure so that we could compare to our exact multipole results; however, the formalism, the FDTD approach, and our conclusions apply to structures of any dimension. Thus the effects discussed in this work should be experimentally seen in suitably designed high-quality high-Q 3D PC slab structures, similar to those recently used in the observation of Rabi splitting [6]. We finally note that our results can be extended to calculate efficiently a projection of the *full complex Green tensor*, which can be used to simplify the understanding and calculation of Rabi splitting [6] and scattering due to roughness [16] in coupled-cavity dielectric microstructures.

This work was produced with the assistance of the Natural Sciences and Engineering Research Council of Canada and the Australian Research Council under the ARC Centres of Excellence program.

*Permanent address: Department of Physics, Queen's University, Kingston, ON, K7L 3N6, Canada.

[1] J. M. Gérard, B. Sermage, B. Gayral, B. Legrand, E. Costard, and V. Thierry-Mieg, Phys. Rev. Lett. **81**, 1110 (1998).
[2] Y. Xu, J. S. Vučković, R. K. Lee, O. J. Painter, A. Scherer, and A. Yariv, J. Opt. Soc. Am. B **16**, 465 (1999).
[3] H. Y. Ryu and M. Notomi, Opt. Lett. **28**, 2390 (2003).
[4] P. Lambropoulos, G. M. Nikolopoulos, T. R. Nielsen, and S. Bay, Rep. Prog. Phys. **63**, 455 (2000).
[5] Y. Xu, R. K. Lee, and A. Yariv, Phys. Rev. A **61**, 033807 (2000).
[6] T. Yoshie, A. Scherer, J. Hendrickson, G. Khitrova, H. M. Gibbs, G. Rupper, C. Ell, O. B. Shchekin, and D. G. Deppe, Nature (London) **432**, 200 (2004).
[7] S. John, Phys. Rev. Lett. **58**, 2486 (1987).
[8] E. Yablonovitch, Phys. Rev. Lett. **58**, 2059 (1987).
[9] J. P. Dowling and C. M. Bowden, Phys. Rev. A **46**, 612 (1992).
[10] R. K. Lee, Y. Xu, and A. Yariv, J. Opt. Soc. Am. B **17**, 1438 (2000).
[11] We consider only atoms with homogeneous linewidths much narrower than the cavity-resonance linewidth.
[12] E. M. Purcell, Phys. Rev. **69**, 681 (1946).
[13] D. P. Fussell, R. C. McPhedran, and C. M. de Sterke, Phys. Rev. E **70**, 066608 (2004).
[14] The boundary radius is chosen by increasing it until just before the point where new resonances appear near the boundary.
[15] A. J. Ward and J. B. Pendry, Phys. Rev. B **58**, 7252 (1998).
[16] S. Hughes, L. Ramunno, J. F. Young, and J. E. Sipe, Phys. Rev. Lett. **94**, 033903 (2005).